Third-day road log, from Deming to Victorio Canyon and the southern Florida Mountains

Nancy J. McMillan, Virginia T. McLemore, Jeffrey M. Amato, John W. Hawley, and Katherine A. Giles

2000, pp. 31-44. https://doi.org/10.56577/FFC-51.31

in:

Southwest Passage: A trip through the Phanerozoic, Lawton, T. F.; McMillan, N. J.; McLemore, V. T.; [eds.], New Mexico Geological Society 51 st Annual Fall Field Conference Guidebook, 282 p. https://doi.org/10.56577/FFC-51

This page is intentionally left blank to maintain order of facing pages.

THIRD-DAY ROAD LOG, FROM DEMING TO VICTORIO CANYON AND THE SOUTHERN FLORIDA MOUNTAINS

NANCY J. McMILLAN, VIRGINIA T. McLEMORE, JEFFREY M. AMATO, JOHN W. HAWLEY, and KATHERINE A. GILES

SATURDAY, OCTOBER 21, 2000

Assembly point: Parking lot of the Grand Hotel, Deming, NM
Departure time: 8:00 a.m.
Distance: 61.3 mi
Stops: 2

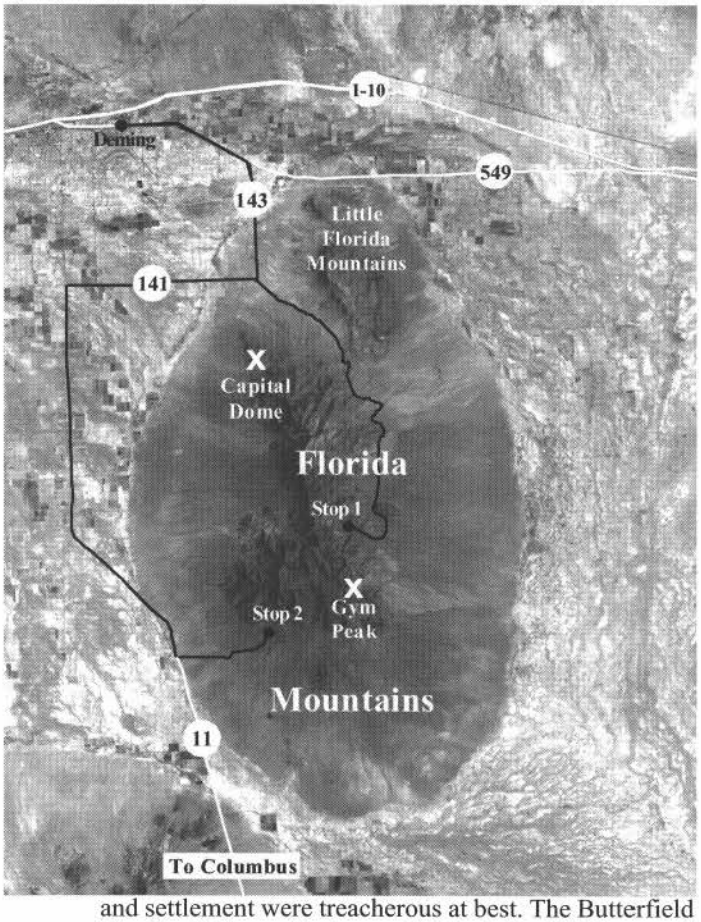

SUMMARY

The third-day tour will circumnavigate the Florida Mountains, a Basin-and-Range horst surrounded by well-developed alluvial fans. The route approaches the Florida Mountains from the north, passing the mid-Tertiary silicic volcanic complex of the Little Florida Mountains and towering spires of volcaniclastic beds of the Eocene Rubio Peak Formation. The nonconformity between basement and Phanerozoic sedimentary rocks takes on several expressions in the Florida Mountains. As the route proceeds south on the east side of the range, the nonconformity first appears between the Eocene Lobo Formation and the Cambrian Florida Mountains intrusion; farther to the south (and at Stop 1), the nonconformity is formed by Ordovician Bliss Sandstone on top of the intrusion.

Nestled in the eroded top of the Florida Mountains intrusion, Victorio Canyon provides the opportunity to discuss evidence for a major magmatic-tectonic event in New Mexico and Colorado during Cambrian–Ordovician time and its possible impact on the geologic history of the region at Stop 1. The traverse crosses the upper eroded surface of the pluton into the overlying Bliss Sandstone and El Paso Limestone of the lower Paleozoic sedimentary succession. The traverse then climbs the canyon wall to reach controversial low-angle faults that have placed deformed El Paso Limestone, Ordovician Montoya Dolomite, and Silurian Fusselman Dolomite on top of the tilted Florida Mountains pluton and its sedimentary cover.

The trip will retrace its path around the north end of the Florida Mountains and drive south on NM-11 on the west side of the range to reach Stop 2. Exposed in the deeper section of the Florida Mountains pluton are examples of magma mixing that formed when mafic magma intruded the partially crystallized, but still mushy, Florida Mountains orthoclase granite.

Mileage

0.0 **Turn left** (east) from the Grand Hotel parking lot onto Pine Street (NM-549, NM-377) to leave Deming. After the Mexican War in 1850, the Americans and Mexicans disputed the southern border of New Mexico that included the area in and around what is now known as Deming. President Franklin Pierce appointed James Gadsden to settle the dispute. The Gadsden Treaty purchase was ratified on April 25, 1854, making southern New Mexico officially part of the United States and providing an important southern route across the country (Clemons et al., 1980).

Deming's success depended on overland travel routes. Because the area was Apache territory, travel and settlement were treacherous at best. The Butterfield Overland Stage Route, established in 1857, passed north of Deming until 1869. It was the longest overland route in its time, beginning in Tipton, Missouri, and ending in San Francisco, California (Conkling and Conkling, 1947). By the 1880s, Deming had grown to the point where it became attractive to the railroads, and in 1881, the Atchinson, Topeka, and Santa Fe (AT&SF) and Southern Pacific (SP) railroads met in Deming. This completed the southern circuit of railroads, providing not only the second transcontinental railroad in the United States but also the only railroad that was open year round. The ensuing rapid settlement of the area led to the eventual subduing of the Apache Indians.

Deming's early years were fairly typical for a western U.S. settlement in the latter part of the nineteenth century. The settlement, consisting mostly of tents, was initially located approximately 10 mi east and was called New Chicago. Better access to water drew the growing village to its current location (Stanley, 1962; Julyan, 1996); irrigation from wells began in 1908 (Darton, 1933). The relocated settlement was named after Mary Anne Deming, the bride of Charles Crocker, who was

one of the founders of the Southern Pacific Railroad (Stanley, 1962; Clemons et al., 1980). E. Germain and Company opened the first store in Deming, using old boxcars for storerooms. The El Paso and Southwestern Railroad also came through Deming, making Deming one of the few towns in New Mexico with depots of three independent railroads. Deming grew quickly and became the center of agriculture and commerce in southern New Mexico. It also attracted cattle rustlers, scalp hunters, and other lawless types (Stanley, 1962). Deming ground water was found to be so pure that it was bottled and shipped to El Paso and other points (Stanley, 1962).

Luna County was established in 1901 from the western portion of Doña Ana County and the eastern portion of Grant County; Deming became the county seat. The county was named after Solomon Luna who sponsored the new county in the legislature.

Deming's significant role in the military history of the region started with Pancho Villa's raid on Columbus on March 10, 1916. Camp Cody was established at Deming in 1917 to train troops for World War I. At the end of the war, Camp Cody was operated by the Catholic Sisters of the Holy Cross as a tuberculosis sanitorium for ex-soldiers. In 1939, Camp Cody was destroyed by fire and the sanitorium closed. The Deming Army Air Base was established in the 1940s for training bombardiers during World War II; it later became the Municipal Deming Airport and Industrial Park.

Today agriculture, especially chili, melons, cotton, and pumpkins, light industry, and tourism are the main economic basis for Deming. But the original resource that drew people to Deming, fresh water, remains a local treasure. **0.3**

0.3 Junction of NM-427, keep straight on NM-529. **1.1**

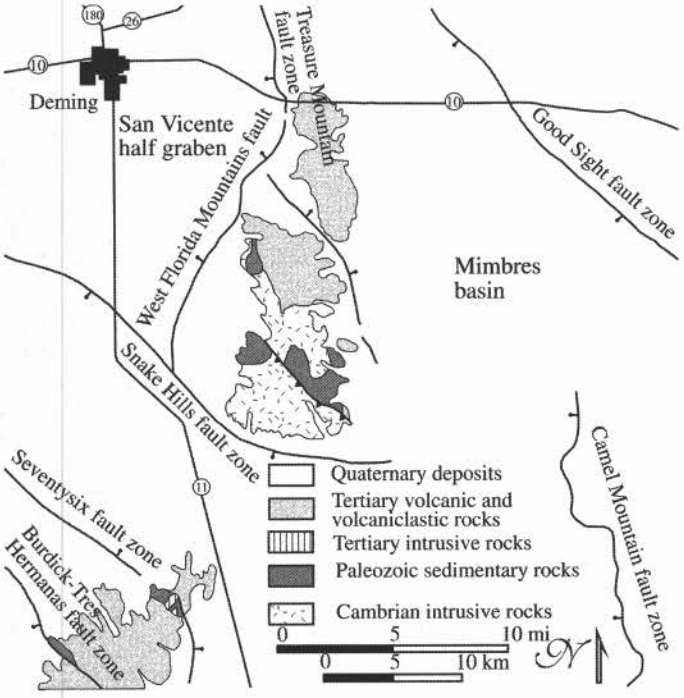

FIGURE 3.1. Generalized map of the Florida Mountains (after Evans and Clemons, 1988; Clemons, 1998; Seager et al., 1995)

1.4 Junction of NM-549 and Business I-10. Continue straight on NM-549 toward Rockhound State Park. Entering area of detailed mapping by Russ Clemons that is synthesized in New Mexico Bureau of Mines and Mineral Resources Memoir 43 (Clemons, 1998). This is also the center of the area originally mapped by Darton (1916, 1917) for the Deming folio of the U.S. Geological Survey geologic atlas series. Deep (up to 12,430 ft) oil and gas exploration wells drilled by Seville-Trident Corporation south and west of the tour route between here and mile 6.5 encountered about 4100 ft of Gila Group basin fill over middle–lower Tertiary volcanic and sedimentary rocks (Clemons, 1986). The No. 1 McSherry Well, located about 1.6 mi west of road log mile 6, penetrated Precambrian gneiss, schist and hornfels(?), and some microcline-bearing granite at 11,828 ft below intrusive monzonite and the lower-Tertiary Lobo Formation. Middle and lower Gila Group conglomerate, mudstone, and sandstone make up most of the basin fill; poorly consolidated deposits of the Upper Gila or Mimbres Formation that comprise the major aquifer zones are no more than 656 to 984 ft thick throughout the Mimbres basin (Darton, 1916; Hanson et al., 1994; Seager, 1995; Haneberg and Friesen, 1995; Hawley et al., 2000). Seager (1995) interprets this part of the Mimbres basin system as a southern extension of the (east-tilted) San Vicente half graben (Fig. 3.1), which is separated from the Cookes Range and Little Florida uplifts by the Treasure Mountain fault zone. The West Florida Mountain fault of Clemons (1998) is a southward continuation of this zone. **1.7**

3.1 Junction of NM-377 (to left) and NM-549, continue right on NM-549. **1.5**

4.6 St. Claire winery on left. **1.1**

5.7 Junction NM-143, just past MP-4. **Turn right** (south) onto NM-143. Dragon Ridge at 12:00 is composed of volcaniclastic conglomerate and sandstone of the Rubio Peak Formation. The Rubio Peak volcanic field erupted dominantly calc-alkaline andesite that post-date Laramide deformation and magmatism but preceded eruptions of mid-Tertiary ignimbrites, mapped in southern New Mexico as the Bell Top Formation. Lawton and McMillan (1999) and McMillan et al. (in press) interpret the Rubio Peak Formation and correlative volcanic rocks as a record of the volcanic arc produced over the Farallon plate as it steepened after Laramide flat-slab subduction. **3.5**

9.2 Cross West Florida Mountains fault, here buried by upper Quaternary piedmont deposits. Clemons (1998) estimated that about 7003 ft of vertical displacement occurred on this major basin-bounding fault during middle to late Cenozoic time. He also noted that the Florida fault-block uplift has been tilted about 23° to the northeast since deposition of the Eocene Rubio Peak Formation. **0.3**

9.5 Junction of NM-143 with B-026 (Rockhound Road, to west) and dirt road. **Turn left** to stay on paved road (Stirrup Road, NM-143). Geode Rock Shop on left. Little Florida Mountains at 10:00 (Fig. 3.2) consist of upper Tertiary fanglomerate and mid-Tertiary rhyolites and rhyolitic ash-flow tuffs overlying andesitic lavas correlated to the Rubio Peak lavas in the Cookes Range

FIGURE 3.2. Little Florida Mountains, looking northwest from Florida Gap.

to the north (Clemons, 1982, 1998). K/Ar age determinations on biotites of 37.3 ± 1.4 Ma from the tuff cropping out west of the Little Gap and 32.0 ± 1.2 Ma from tuff one mile north of Rockhound State Park (Clemons, 1982), and a new $^{40}Ar/^{39}Ar$ age determination of 33.5 ± 0.2 Ma on biotite on the ash flow tuff at the base of the section (McLemore et al., this road log) do not correlate with the ages of regional Oligoene ash-flow sheets (McIntosh et al., 1991). $^{40}Ar/^{39}Ar$ age determinations on the groundmass of rhyolite and andesite of the Little Floridas and of a rhyolite dike in Spring Canyon in the northern Florida Mountains are considerably younger (28.5–24.4 Ma, McLemore et al., this road log). **1.6**

11.1 **Sharp turn to the left. 0.3**

11.4 Junction of NM-143 (road to Rockhound State Park) with NM-198 (road to Spring Canyon Park). **Turn right** on NM-198. **0.6**

ROCKHOUND STATE PARK AND SPRING CANYON RECREATION AREA

Virginia T. McLemore, Nelia W. Dunbar and William C. McIntosh

New Mexico Bureau of Mines and Mineral Resources, New Mexico Institue of Mining and Technology, 801 Leroy Pl., Socorro, NM 87801; ginger@gis.nmt.edu

Rockhound State Park lies in the Little Florida Mountains southeast of Deming, New Mexico. It was established in 1966 as the first park in the United States that allowed collecting of rocks and minerals for personal use. Each visitor is allowed to collect as much as 15 lbs of rocks and minerals from the 250-acre park; mineral dealers are not allowed to collect for sale. Rockhound State Park actually consists of two separate sites, the main park in the Little Florida Mountains and Spring Canyon Recreation Area in the northern Florida Mountains. The main park offers covered shelters for camping and picnicking, a group shelter, restrooms with showers, RV dump station, playground, hiking trails, wildlife viewing areas, and rock and mineral collecting. Spring Canyon lies in the northern Florida Mountains, south of the main park, and is open for day use only. Facilities include picnic tables, restrooms, and hiking trails.

Prehistoric people most likely camped thousands of years ago beneath rocks that provided some shelter from the elements and predators. The Mimbres or Mimbreno Indians settled north of the area about A.D 1200–1150. Arrowheads and pottery shards are still found today and remind us of their former presence. Later, Apache Indians moved into the area. The rugged Florida Mountains were well known as Apache strongholds until the mid-1880s. Spanish conquistadors and settlers traveled through the area in the 1500s, but did not find the desert environment or the Apache Indians very hospitable. Spanish explorers named the larger range in the 1700s. The range was shown on Juan Nentwig's map of 1762 as Sierra Floridas (Julyan, 1996). In 1804, Col. Manuel Carrasco, a Spanish army officer, began mining the copper at Santa Rita (McLemore, 1996a). Mule trains loaded with copper from the mine passed near what is now the state park, on their way to Chihuahua in 1804–1834 (Weber, 1980).

The Little Florida Mountains consist predominantly of interbedded mid-Tertiary andesite, dacite, ash-flow tuff, rhyolite, and fanglomerate intruded by rhyolite domes and dikes (Clemons, 1982, 1984, 1998; Clemons and Brown, 1983). Altered sanidine and biotite from an ash flow near the base of the stratigraphic section at Little Gap give $^{40}Ar/^{39}Ar$ ages of 33.5 ± 0.2 Ma and 32.9 ± 0.2 Ma, respectively. This ash flow may correlate with the 33.5 Ma Oak Creek Tuff, erupted from the Juniper caldera in the northern Animas Range in the Boot Heel volcanic field (McIntosh and Bryan, this volume). Additional rhyolite and andesite samples from the state park range in age from 24.4 ± 0.4 to 28.5 ± 0.3 Ma (groundmass, $^{40}Ar/^{39}Ar$; this report). A rhyolite dike at the head of Spring Canyon has been dated as 25.4 ± 0.7 Ma (groundmass, $^{40}Ar/^{39}Ar$; this report).

Gray perlite, thundereggs, jasper, onyx, geodes, agate, rhyolite, and quartz crystals are among the more common minerals and rocks found in the park. Thompsonite, a zeolite, is found in amygdules in quartz latite (Northrop and LaBruzza, 1996). Agate is present in a wide range of colors, and is one of the minerals that many visitors collect at Rockhound State Park. Some geodes found at Rockhound contain multicolored agate in addition to well-formed quartz crystals.

One of the geologically interesting features of Rockhound State Park is the presence of numerous spherulites within the rhyolite lava. Many of these spherulites have cores that contain agate or quartz crystals. The spherulites range in size from <0.04 in. to >1 ft. When broken open, the spherulites exhibit distinct concentric banding, as well as numerous silica-filled fractures and open-space filling silica. In order to gain some insight into the process by which these spherulites form, samples were examined using back-scattered electron imaging and qualitative X-ray analysis and imaging using a Cameca SX-100 electron microprobe. The imaging and X-ray analysis show that the spherulites are formed of bands of pure quartz intermixed with bands of intergrown feldspar and quartz (Fig. 3.3). This banding produced the concentric appearance of the spherulites. Bands of quartz crosscutting the banded structure are also observed (Fig. 3.3).

The observed patterns in the spherulites suggest that they formed dur-

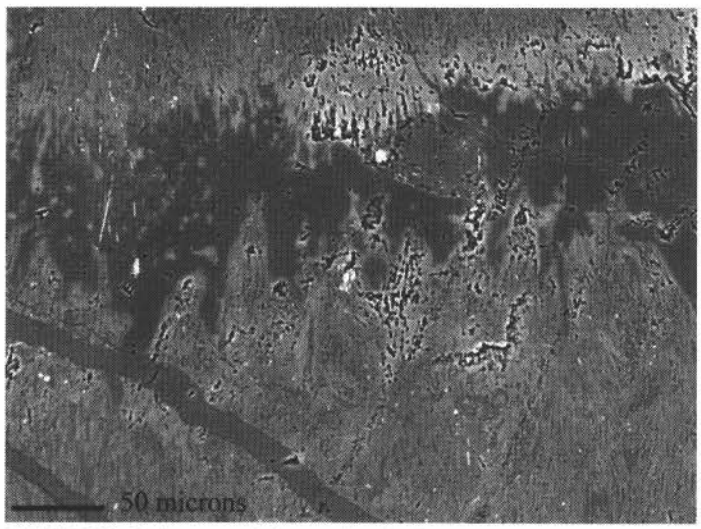

FIGURE 3.3. Back-scattered electron image of a polished slab of a spherulite. The dark gray, seen both in bands and veins, is quartz. The lighter gray shade represents alkali feldspar. The dark gray intermixed with the lighter gray shade represents intergrowth of quartz and alkali feldspar.

ing the cooling of the rhyolite lava. Similar spherulitic features were observed in an artificial melt that was rapidly cooled (Jacobs et al., 1992; Dunbar et al., 1995). The temperature of the artificial melt was monitored during the cooling process, and exothermic crystallization was observed at high temperatures (2000°F). Spherulitic growth occurred during this crystallization process, and the internal structure of the spherulites was indistinguishable from the internal structure of Rockhound spherulites, although in the artificial melt the phenocryst phases were plagioclase and pyroxene rather than quartz and alkali feldspar. This similarity suggests that the Rockhound spherulites formed by a high-temperature magmatic crystallization rather than by sub-solidus processes. The quartz veins and agate associated with the spherulites formed later, as evidenced by the cross-cutting relationships of the hydrothermal quartz with the igneous quartz and feldspar.

12.0 Junction of NM-198 with gravel road to Spring Canyon Park. Leave paved road; **continue straight on gravel road B023** through Florida Gap between the Little Florida Mountains and the Florida Mountains. The Florida Mountains mining district, discovered in 1876, is located south of Spring Canyon in the main Florida Mountains. From 1880 to 1956, 5000 lbs Cu, <10 oz Au, 8000 oz Ag, and >30,000 lbs Pb worth approximately $102,000 were produced from carbonate-hosted Pb-Zn and polymetallic vein deposits in the district (McLemore et al., 1996b). The Mahoney and Silver Cave mines were the largest metal producers. In addition, 200 short tons (st) of fluorite and 1421 long tons of 22–30% Mn have been produced from epithermal veins in the area (Farnham, 1961; McLemore et al., 1996b). Manganese was mined from veins on the southeast slopes during the Government purchasing program in the 1950s (Gundiler, this volume, p. 279). **1.2**

13.2 **Sharp right turn in gravel road**. Spires at 12:00 (Fig. 3.4) are columns of Rubio Peak volcaniclastic rocks of Castle Rock. **0.4**

13.6 **Sharp left bend in gravel road** at brick ranch house. **0.2**

13.8 Junction with gravel road. **Continue straight over cattle guard and cross onto Tres Lomitas ranch**. Radio tower on left. The ridge at 12:00 is a piedmont slope on the Quaternary Mimbres Formation. **0.2**

14.0 Fork in road; **take left fork**. Entering the Florida Mountains Wilderness Study Area—**stay on roads**. **1.5**

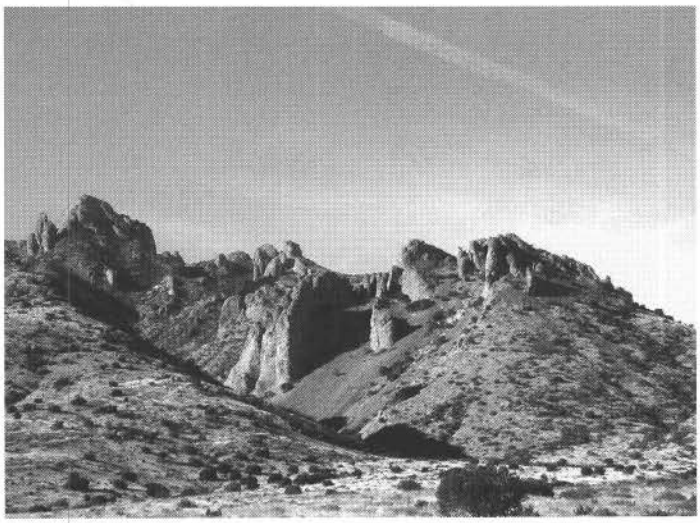

FIGURE 3.4. Spires of Eocene Rubio Peak Formation in the northern Florida Mountains, looking south from Florida Gap.

15.5 Cattle guard. **0.1**

15.6 Cattle guard. Across the Mimbres basin, the Quaternary Potrillo basalt field is visible at 12:00, mid-Tertiary granites, syenites, and tuffs in the Organ Mountains (Seager, 1981) at 11:00, and mesas of mid-Tertiary Bell Top tuffs capped by Uvas basaltic andesite in the Sierra de las Uvas at 10:00. **0.1**

15.7 Junction with dirt road on right; **continue straight** (left fork). **1.0**

16.7 Junction with dirt road on right; **continue on main road to the left**. High peak at 1:00 is Florida Peak (elevation 7448 ft.) in the Rubio Peak Formation. The dirt road on the right is the road to the Bradley Mine. **0.5**

17.2 Junction with dirt road on left; **continue to right** on the main road. **0.3**

17.5 North-dipping bedded volcaniclastic rocks of the Rubio Peak Formation at 3:00. **0.6**

18.1 Junction with dirt road on right to windmill. **Continue on main road to the left**. On the skyline at 3:00, the nonconformity between the Eocene Lobo Formation on top of the Cambrian Florida Mountains intrusion is exposed. The Lobo Formation in the Florida Mountains accumulated in intramontane basins between west–northwest-trending, Laramide basement-cored uplifts (Mack and Clemons, 1988). The southernmost of these basins (now exposed in the northern Florida Mountains) contains a well-preserved unroofing sequence that grades upward from a clast population dominated by Paleozoic formations to an abundance of K-feldspar and plagioclase grains with quartzofeldspathic and low-grade metamorphic clasts. This unroofing sequence is overlain by volcanic litharenite with andesitic clasts indicating the onset of Rubio Peak volcanism (Mack and Clemons, 1988). **0.1**

18.2 Cattle guard. **0.2**

18.4 Crossing drainages from the east side of the Floridas. At 11:30 are the Three Little Hills, which consist of the Starvation Draw Member of the Rubio Peak Formation overlying the Lobo Formation. Gym Peak (elevation 7104 ft.) is at 12:00; the cliffs of Baldy Peak (7106 ft) at 1:00 (Fig. 3.5) are formed in Ordovician El Paso Group carbonates that structurally overlie Cambrian syenite along controversial low-angle faults (Amato, this volume). At 12:30 are the San-Tex mines. **0.3**

18.7 Road fork. **Take left fork.** **0.1**

18.8 Junction with dirt road on the left. **Continue straight** on main dirt road. **0.2**

19.0 Junction with dirt road on the right. **Continue straight** (left fork) on the main dirt road. **0.8**

19.8 Junction with dirt road on the right. **Take left fork**. Crossing the west end of the Three Little Hills. **0.1**

19.9 Fork in dirt road. **Take left fork**. Driving along the south edge of the Three Little Hills. **0.5**

20.4 Sharp right turn, Junction with road on left. **Take the right turn,** continuing on main dirt road. **0.2**

20.6 Pass through gate. Calcic soils in young piedmont deposits along road. **0.1**

20.7 Junction with road on right. **Continue on the left fork** toward the south. Knob at 1:00 is Fusselman Dolomite, the sentinel to Victorio Canyon. The mine dump on

FIGURE 3.5. Baldy Peak (cliffs to the left of center) consists of Ordovician El Paso Limestone faulted on top of the Cambrian Florida Mountains intrusion.

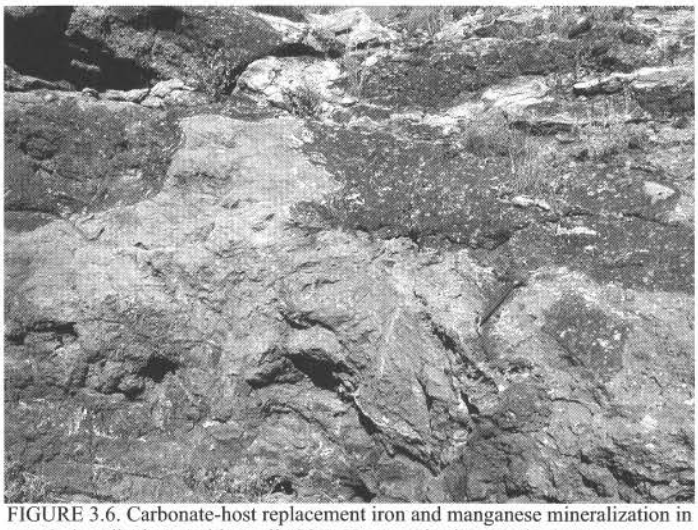

FIGURE 3.6. Carbonate-host replacement iron and manganese mineralization in trench described at road log mile 20.7. Hammer is about 15 in. long.

right is in brecciated and mineralized Ordovician Montoya Formation. The trench is approximately 160 ft long, with little, if any, production. A nice contact between the carbonate-hosted replacement deposit and the barren limestone, typical of oxidized carbonate-hosted replacement deposits throughout southwest New Mexico, is exposed in the trench (Fig. 3.6). The mineral assemblage consists of iron and manganese oxides and hydroxides, silica minerals, and brown and gray jasper. Late-stage calcite fills some of the gas cavities. No evidence for sulfide or relic sulfide mineralization is present. Rare clasts of rhyolitic ash-flow tuff and possible volcanic/volcaniclastic rocks from the Rubio Peak Formation(?) suggest that the deposit may be Eocene–mid-Tertiary in age and related to local volcanism. **0.4**

FLORIDA MOUNTAINS MINING DISTRICT, LUNA COUNTY, NEW MEXICO

Virginia T. McLemore

New Mexico Bureau of Mines and Mineral Resources, New Mexico Institute of Mining and Technology, 801 Leroy Pl., Socorro, NM 87801

The Florida Mountains district, discovered in 1876, is located east of Deming and includes only the main Florida Mountains, south of Florida Gap. The district is adjacent to the Florida Mountains Wilderness Study Area. From 1880 to 1956, 5000 lbs Cu, <10 oz Au, 8000 oz Ag, and >30,000 lbs Pb worth approximately $102,000 were produced from carbonate-hosted replacement Pb-Zn and polymetallic vein deposits in the district (Griswold, 1961; McLemore et al., 1996b). The Mahoney and Silver Cave mines are the largest metal producers. In addition, 200 short tons (st) of fluorite and 1421 long tons (lt) of 22–30% Mn have been produced from epithermal veins in the area (Rothrock et al., 1946; Farnham, 1961; McLemore et al., 1996b). Manganese was mined from veins on the southeast slopes during the Government purchasing program in the 1950s (see Gundiler, "Brief history of Deming area mills and manganeses stockpiles," this volume, p. 279).

The Florida Mountains form the northern portion of the Laramide thrust belt as defined by Drewes (1991) and are along the Texas lineament. Rocks in the area consist of Paleozoic through lower Tertiary sedimentary rocks overlying Proterozoic metamorphic rocks and Cambrian granite and syenite plutons (Clemons and Brown, 1983; Clemons, 1984). Tertiary rhyolite, diorite, and andesite intrudes the older lithologies; a rhyolite west of Florida Peak was dated as 29.1 ± 1.3 Ma (feldspar, K-Ar; Clemons and Brown, 1983). Laramide tilting, thrusting and uplift, followed by Tertiary Basin-and-Range uplift have deformed the rocks.

Carbonate-hosted replacement Pb-Zn and polymetallic vein deposits occur throughout the district (McLemore et al., 1996b). The carbonate-hosted deposits are typically in Fusselman Dolomite and follow fracture and/or fault zones. The deposits occur as fissure veins or manto-replacement bodies that contain smithsonite, cerussite, malachite, azurite, barite, quartz, calcite, and local galena and sphalerite (Griswold, 1961). Lead typically exceeds zinc and copper in abundance. The deposits are typically small, <2 m wide and several hundred meters long.

Polymetallic veins occur along fractures and faults within Proterozoic granite, Precambrian–Cambrian syenite, and Tertiary agglomerate (McLemore et al., 1996b). The Park mine occurs along a fault separating Proterozoic granite and Paleozoic sedimentary rocks. Production from these veins has been small, but locally, they are higher in grade than the carbonate-hosted replacement Pb-Zn deposits. The veins are typically <2 m wide, several hundred meters long, of variable dips, and contain quartz, pyrite, calcite, iron and manganese oxides, chalcopyrite, and local galena, sphalerite, fluorite, and barite.

Fluorite occurs as veins, void fillings, and replacements of limestones. Breccias and jasperoids are common. Most of the fluorite veins and fissures occur along faults and fractures. Fluorite and quartz are the predominant minerals in a gangue of calcite, clay, and rare barite and pyrite. Fluid inclusion data of fluorite from the Florida Mountains indicates formation from low temperature (146–194°C) and low salinity (6.2–8.4 eq. wt.% NaCl) fluids, suggesting a meteoric origin (North and Tuff, 1986).

The Waddell Atir mine was first prospected in 1910 (Williams et al., 1964), but there is no reported production. In 1980, Barite Corporation of America drove a 236.2-m-long adit to intersect the vein, but did not find enough ore to produce. The vein strikes N60°E and dips 55°SE and consists of barite, fluorite, galena, calcite, and quartz. It is 1.5–3.6 m wide and 61 m long and occurs in Cambrian syenite. A sample assayed 41% $BaSO_4$, 19.7% CaF_2, and 1.8% Pb (Williams et al., 1964).

Epithermal and carbonate-hosted manganese deposits occur throughout the Florida Mountains. The veins and replacements are typically small; veins are generally <1 m wide and the largest replacement deposits at the Birchfield mine are only 2.3 m wide. The deposits follow bedding planes, which strike northeast. Locally, the deposits form cross cutting pipe-like bodies, i.e., chimneys.

The potential for additional barite-fluorite and manganese deposits in the Florida Mountains is probably good, but not likely to be produced in the near future because of poor market conditions. Additional carbonate-hosted Pb-Zn and vein deposits are likely to be found along strike of most deposits.

21.1 Junction with dirt road on right to San-Tex mines.

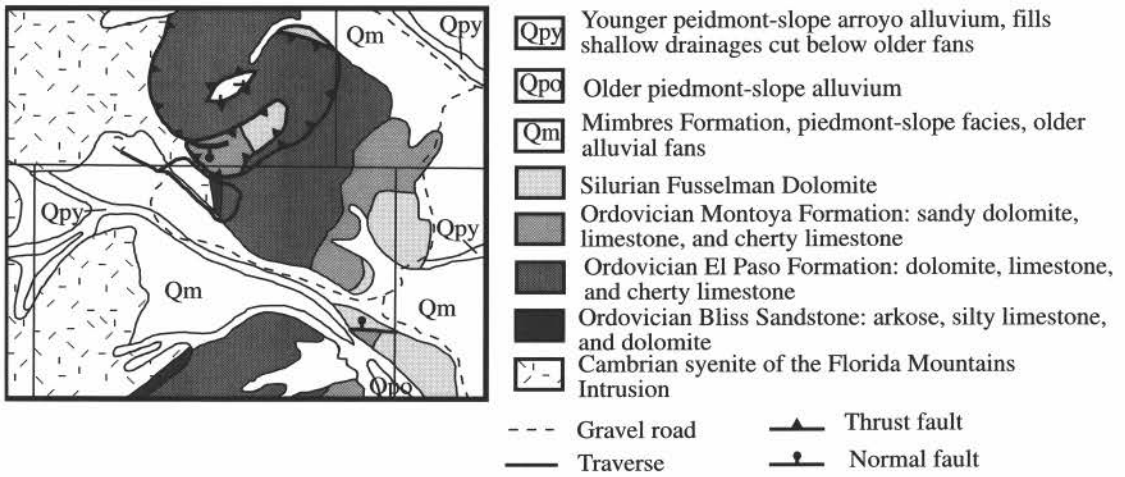

FIGURE 3.7. Simplified geologic map of Victorio Canyon, after Clemons and Brown (1983).

Continue on the left fork. **0.1**

21.2 Junction with dirt road on right. **Turn right** (west) into Victorio Canyon. Hills of El Paso Limestone on both sides in the narrows of the canyon. The canyon widens out into the Cambrian Florida Mountains intrusion, nonconformably overlain by the Cambrian–Ordovician Bliss Sandstone. **0.8**

22.0 Junction with dirt road. **Take the right fork** down into Victorio Draw. **0.1**

22.1 Boundary marker on left (SE¼ sec. 31, T25S, R7W). **0.2**

22.3 **STOP 1. Pull around loop at corral.** Victorio Canyon in the Florida Mountains provides an opportunity to examine the Cambrian Florida Mountains intrusion, the nonconformity between the intrusion and the Ordovician Bliss Sandstone, and the overlying El Paso Limestone (Fig. 3.7). Low-angle faults on the north side of the canyon place the Ordovician El Paso Limestone and Montoya Formation and the Silurian Fusselman Dolomite on top of the intrusion, Bliss Sandstone, and El Paso Limestone.

On foot, follow Victorio Draw to the west. Walk through upper part of the Florida Mountains intrusion (syenite). Dikes of fine-grained syenite intrude the pluton, and are probably also Cambrian in age. The dikes are truncated on their northern end by the low-angle faults exposed on the hillside. The pluton-Bliss Sandstone nonconformity is well exposed in the arroyo (Fig. 3.8). Large clasts (5 ft in diameter) of syenite in the Bliss Sandstone (Fig. 3.9) suggest that knobs of the syenite existed as sea stacks surrounded by Bliss sands during early Paleozoic transgression. Continuing to walk westward, note that the Bliss arkose grades rapidly into dolomite and limestone of the Lower Ordovician El Paso Group (Bowen Formation). The carbonates comprise thinly bedded packstone–grainstone containing silicified echinoderm debris intercalated with fine-grained arkose stringers. Beds thicken upward into burrowed wackestone and packstone with chert horizons and progressively fewer siliciclastic interbeds. Carbonates contain ripple cross-laminae, basal rip-up conglomerate layers, flaser bedding, and algal laminites with local stromatolitic heads. The stratal assemblage indicates deposition within a peritidal environment with the lower beds deposited in a high-energy beach/shoreline zone overlain by tidal flat facies. Turn northward

FIGURE 3.8. Ordovician Bliss Sandstone nonconformably overlying the Cambrian Florida Mountains intrusion. The Bliss Sandstone dips approximately 45° to the right. Hammer is about 15 in. long.

FIGURE 3.9. Large clast of Cambrian syenite in Bliss Sandstone. Hammer is about 15 in. long.

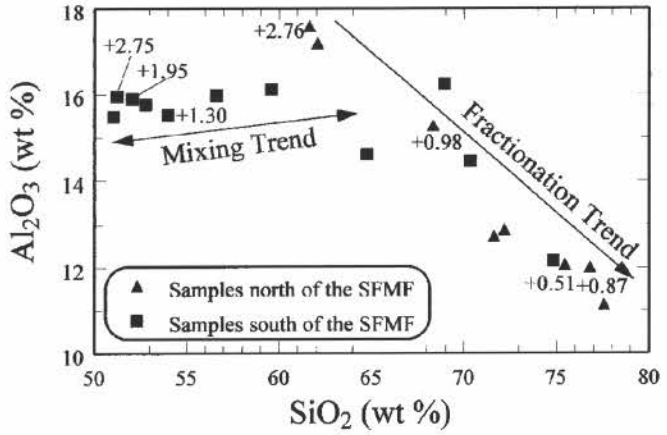

FIGURE 3.10. SiO_2-Al_2O_3 for samples from the Florida Mountains intrusion. Small numbers associated with some data points give the ε_{Nd} values calculated at 511 Ma for those samples. ε_{Nd} values describe the $^{143}Nd/^{144}Nd$ ratio of a sample relative to the $^{143}Nd/^{144}Nd$ of bulk earth at the age of the sample. Values near zero are near bulk earth; positive values reflect an incompatible element-depleted source (mid-ocean ridge mantle, for example). Negative values indicate an incompatible element-enriched source.

and climb up to observe low-angle faults (Brown, 1982; Amato, this volume). Walking downhill to return to the caravan, notice that the floor of Victorio Canyon was once covered with thin alluvial-fan and coalescent-fan deposits of the Quaternary Mimbres Formation. The Mimbres Formation is correlative to the Camp Rice Formation and accumulated to a thickness of several thousand feet in the Mimbres basin to the east of the Florida Mountains. Mimbres fans have been dissected by modern arroyos that are less than 25,000 yrs old (Clemons, 1998).

Petrographic, geochronologic, geochemical, and isotopic study of the Florida Mountains intrusion has resolved several controversies surrounding the origin of the intrusion (Ervin, 1998) but opened new speculation concerning the Cambrian tectonics of New Mexico and Colorado (McMillan et al., this volume). One important question concerned offset on the south Florida Mountains fault (SFMF) (Fig. 3.1), a major steeply dipping reverse fault that places Cambrian alkali-feldspar granite on Cambrian syenite and lower Paleozoic sedimentary rocks. Ervin (1998) demonstrated that plutonic rocks throughout the Florida Mountains have similar

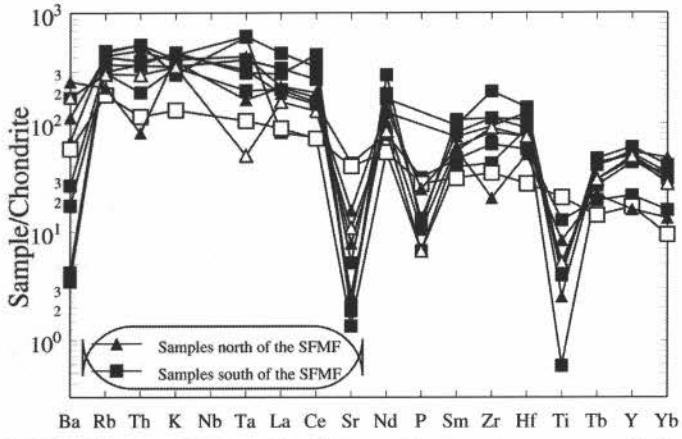

FIGURE 3.11. Chondrite-normalized incompatible trace-element patterns for the Florida Mountains intrusion. Open square = mafic enclave from southern Florida Mountains. Open triangle = unusual sample with low Ta.

major element, trace element, and Nd isotopic compositions, data that argue against major offset across the SFMF.

The trace element and isotopic composition of the Florida Mountains intrusion are useful for more than correlating the pluton across the SFMF. Two trends are clear on major element diagrams (Fig. 3.10). The major differentiation trend, from syenite at about 60% SiO_2 to alkali-feldspar granite at 78% SiO_2, is defined by decreasing Al_2O_3, Na_2O, and K_2O with increasing SiO_2, which indicates that fractional crystallization of K-feldspar was an important differentiation process. However, the fractionation trend shows small but measurable changes in ε_{Nd} from +2.76 at the syenite end to +0.5 at the evolved end, suggesting that fractionation was accompanied by a small amount of assimilation. The second trend comprises samples of hybrid rocks from the zone of magma mixing in the southern part of the pluton. Hybrid rocks form a linear trend from mafic (ca. 51% SiO_2) to syenite (ca. 65% SiO_2). The textures that indicate magma mixing will be examined at Stop 2. The ε_{Nd} values of the most mafic magmas in the mixed zone are between +2 and +3, similar to the most mafic syenite. The syenites likely evolved by fractional crystallization from mafic magmas similar to those frozen as mixed enclaves. The syenitic magma then moved upward in the crust and evolved by assimilation-fractional crystallization to alkali feldspar. During crystallization, the base of the chamber was intruded by mafic magma, which mixed with granitic magma to form the hybrid plutonic rocks.

The tectonic setting in Cambrian time in southern New Mexico must allow for mantle-derived magmatism. The trace element composition of the Florida Mountains intrusion provides a hint concerning the tectonic environment. Arc magmas, and thus much of the continental crust, have low Nb and Ta, forming a trough at these elements on chondrite-normalized incompatible trace element diagrams (Fig. 3.11). In stark contrast, almost all of the Florida Mountains intrusion samples are either flat, very mildly low, or have peaks at Nb and Ta (Ervin, 1998), precluding subduction or remelting of older arc rocks as the origin of the magmas. Rather, it is likely that the mafic magmas were generated by partial melting of the mantle during continental rifting or interaction with a mantle plume. In either case, the pluton was probably emplaced during continental extension. McMillan et al. (this volume) suggest that the Florida Mountains intrusion is one of many Cambrian intrusive suites in New Mexico and Colorado produced within an aulacogen.

CAMBRIAN TECTONICS OF NEW MEXICO AND COLORADO

Nancy J. McMillan[1], Virginia T. McLemore[2], and Sheryl D. Erwin[3]

[1]Department of Geological Sciences, New Mexico State University, Las Cruces, New Mexico, 88003, nmcmilla@nmsu.edu; [2]New Mexico Bureau of Mines and Mineral Resources, New Mexico Tech, 801 Leroy Place, Socorro, New Mexico 87801, ginger@gis.nmt.edu; [3]Texaco, Midland, Texas

A suite of alkaline igneous rocks of latest Precambrian–Ordovician age in New Mexico and Colorado indicates that the region's tectonic

history is more complicated immediately prior to deposition of the early Paleozoic passive-margin sequence than previously thought. Only a few of these rocks have been well dated (Table 3.1), but similarities in field relationships and geochemistry suggest a common tectonic affinity. The igneous rocks are preserved as plutons, dike swarms, and small intrusions of syenite and carbonatite; many of the syenites and their host rocks have experienced potassium metasomatism that caused loss of nearly all Na_2O and CaO and addition of K_2O (typically 12–15 wt. %). Published whole-rock analyses of syenites suggest that they could have two different origins. One suite, with high Ta and Nb concentrations, probably fractionated from mantle-derived mafic magma. The Florida Mountains intrusion falls into this category. The other, more common, geochemical signature is arc-like, with low Nb and Ta relative to other incompatible trace elements. These probably represent partial melts of crustal rocks; however, the heat of melting must have been supplied from the mantle, either by conduction from hot, convecting mantle or by intrusion of mantle-derived mafic magma. Significant mantle perturbation and tectonic activity are implied by either case and the presence of carbonatites.

Data from the Florida Mountains intrusion provide information that supports the hypothesis of regional Cambrian tectonic activity (Ervin, 1998). Chondrite-normalized incompatible trace-element patterns (Fig. 3.11) exhibit flat or concave-downward trends at Nb and Ta for all but one sample, suggesting that the syenites and granites fractionated from a mantle-derived basalt. Mafic enclaves involved in magma mixing at the base of the pluton (see Stop 2) have compositions that could represent the parental mafic magmas of this system (open square in Fig. 3.11). This trace element pattern, coupled with ε_{Nd} values of enclaves and granite between +2.8 and +0.5 (calculated at 511 Ma, Ervin, 1998), is consistent with derivation from a mantle plume or in a continental rift.

Additional evidence for tectonic activity comes from a comparison of geochronologic data from the pluton with the age of the Ordovician Bliss Sandstone, which nonconformably overlies the pluton. Two U-Pb zircon-crystallization ages have been published: 503 ± 10 Ma (Evans and Clemons, 1988) and 514 ± 3 Ma (Matheny et al., 1988). These overlap at ca. 511 Ma, which we interpret as the crystallization age of the pluton. $^{40}Ar/^{39}Ar$ analyses on biotite and hornblende from the syenite yielded a biotite-plateau age of 490.5 ± 5.4 Ma and a less rigorous hornblende-plateau age of 485.5 ± 4.9 Ma (Ervin, 1998). We interpret the biotite age to mean that the pluton was exhumed and passed through the 300–350°C closure temperature of biotite (Harrison et al., 1985) at approximately 491 Ma, some 20 Ma after crystallization. If this interpretation is correct, the pluton was intruded at a depth where the temperature was greater than 300–350° C. Assuming an average cratonal geotherm of 25°C/km, the pluton crystallized at a depth greater than 12–14 km; a steeper geotherm lowers the minimum depth of intrusion but implies heat transfer to the crust by processes in addition to simple conduction. The lack of good biostratigraphic fauna in the Bliss Sandstone make it difficult to date; however, the overlying El Paso Limestone is Early Ordovician in age (Canadian, Clemons, 1998). The duration of the Early Ordovician is now thought to be 490–470 Ma (Cowie and Bassett, 1989). Using depths of intrusion from 14 to 7 km and depositional ages for the Bliss from 480 to 470 Ma, average long-term exhumation rates for the region range from 1.3 mm/yr to 0.3 mm/yr. Although these rates are low for exhumation caused by tectonic activity (Blythe, 1998; Amato, 1999), the fact that measurable

Table 3.1. Known and possible Cambrian–Ordovician carbonatites and alkaline igneous rocks in New Mexico and Colorado. Locations are shown on Figure 3.12. References in the table can be found in McLemore et al. (1999a).

Area	Lithology	Age (Ma)	References
McClure Mountains	carbonatite-alkaline complex	517–704 (K-Ar, Rb-Sr, fission track)	Fenton and Faure (1970), Olson et al. (1967), Armbrustmacher (1984)
Democrat Creek	syenite	520–546 (K-Ar, Rb-Sr, fission track)	Olson et al. (1977), Armbrustmacher (1984)
Gem Park	carbonatite, syenite	?	Olson et al. (1967), Armbrustmacher (1984)
Iron Hill	carbonatite	550–579 (K-Ar, Rb-Sr, fission track)	Fenton and Faure (1970), Olson et al. (1977)
Black Canyon of the Gunnison	diabase	495 ± 15 (Rb/Sr), 533 ± 20, 504 ± 16 (K-Ar)	Larson et al., 1985
Sangre de Cristo Mountains	high-Na Syenites	?	Klich (1983), Reed et al. (1983), McLemore (1989)
Nacimiento Mountains	high-K Syenites	?	Woodward et al. (1977), McLemore (1989)
Zuni Mountains	high-Na Syenites	?	Lambert (1983), McLemore and McKee (1989)
Pedernal Hills	high-Na Syenites	469 ± 7 (Rb-Sr)	Loring and Armstrong (1980), McLemore (1984), McKeown (1991), Mukhopadhyay et al., (1975), Jackson et al. (1988)
Lobo Hill (Moriarty)	high-K syenite, monzonites, carbonatite	518 ± 5.7 ($^{40}Ar/^{39}Ar$)	Loring and Armstrong (1980), McLemore (1984), McKeown (1991), McLemore et al. (1999a)
Monte Largo (Sandia Mountains)	carbonatites, melterzite sill	?	Lambert (1961), McLemore (1984)
Lemitar Mountains	carbonatites	457 ± 16 (K-Ar, biotite)	McLemore (1982, 1983, 1987a), McLemore and Modreski (1990)
Chupadera Mountains	carbonatites	?	Kent (1982), McLemore (1987a), Van Allen et al. (1986)
Caballo Mountains	high-K syenites	?	Staatz et al. (1965), McLemore (1986)
Florida Mountains	syenite and alkali-feldspar granite	511 crystallization, 491 cooling (U-Pb zircon, $^{40}Ar/^{39}Ar$)	Evans and Clemons (1988), Loring et al. (1987), Matheny et al. (1988, 1990), Clemons (1998), Ervin (1998)
Burro Mountains	high-Na, high-K syenites	?	McLemore and McKee (1988)
Little Hatchet Mountains	alkaline granite	605, 640 (Lead-alpha) zircons	Zeller (1965)
Bent Dome (Sacramento Mts.)	granite, diorite	?	Foord and Moore (1991), Bauer and Lozinsky (1991)
Costilla Creek	diorite dike	500 (whole-rock Rb-Sr)	Reed (1984)
Houston Oil and Minerals Lewelling No. 2 oil test	basalt or andesite	514 ± 21 (K-Ar)	Loring and Armstrong (1980)
Trans-Pecos Resources Latigo Ranch #1A and 1D oil tests	gneiss, feldspar porphyry	720 ± 36, 604 ± 30 (K-Ar)	Setter and Adams (1985)
Yates Petroleum T-4 Cattle Co. #1 and #2 oil test	granite	376 ± 19, 664 ± 35, 766 ± 38 (K-Ar)	Setter and Adams (1985)
Rattlesnake Hills	basalt	848 ± 42 (K-Ar)	Setter and Adams (1985), Setter (1985)

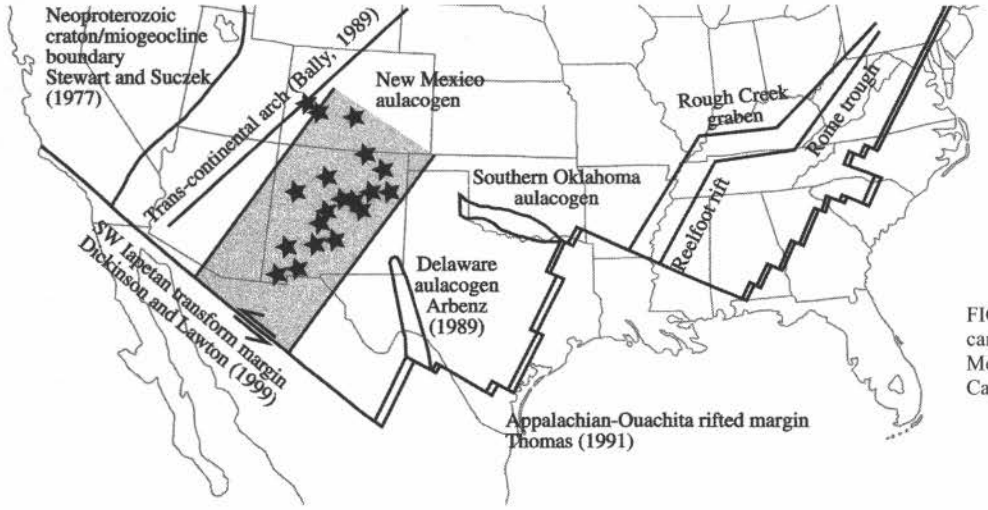

FIGURE 3.12. Location of Cambrian–Ordovician carbonatite and alkaline igneous rocks in New Mexico and Colorado and their relationship to Cambrian tectonic elements.

Cambrian–Ordovician exhumation occurred suggests that the simple passive margin hypothesis be revisited.

Cambrian–Ordovician intrusions of New Mexico and Colorado extend across New Mexico and Colorado in a NNE band (Fig. 3.12) roughly parallel to the rift segments of the southern margin of Laurentia (Thomas, 1991). The New Mexico–Colorado rocks may thus be interpreted as the record of a continental rift , which we call the New Mexico aulacogen, that is similar in origin and orientation to the Reelfoot rift and Rome trough (Kolata and Nelson, 1997). However, the New Mexico aulacogen lacks several of the features that characterize lower Paleozoic extensional basins in the southeastern United States. For instance, the Reelfoot rift consists of deep sediment-filled basins bounded by normal faults. Igneous rocks are not abundant, but broad subsidence of the area during Ordovician time is attributed to cooling of a dense continental root of Cambrian mafic intrusions (Kolata and Nelson, 1997). In contrast, evidence for the New Mexico aulacogen is based on igneous rocks; syn-rift sedimentary rocks are essentially absent. Evidence for Cambrian normal faults has yet to be found. It is interesting that the transcontinental arch, a positive topographic feature that controlled sedimentation patterns in western North America during Paleozoic time (Bally, 1989), coincides approximately with the western margin of the New Mexico aulacogen (Fig. 3.12). It is possible that the New Mexico aulacogen was topographically high due to mantle perturbation, and that syn-rift sediments were transported away from the topographic high. Perhaps the western flank became the long-standing transcontinental arch due to its proximity to the warm, thin, recently rifted western margin of North America.

As you leave Victorio Canyon, you have a magnificent view of over 100 cinder cones of the Quaternary Potrillo Volcanic Field. The basalts of the field and underlying basin fill of the upper Santa Fe Group cover a great variety of older rocks and structures, ranging in age from Precambrian to Neogene. Units include Paleozoic and Mesozoic sedimentary rocks as well as Tertiary volcanic rocks (Seager, 1989, 1995). The broad Florida subbasin of the Mimbres basin system between the Florida and the West Potrillo-Camel Mountain uplifts is bounded on the east by the Camel Mountain fault zone. The Florida subbasin is segmented into several structural subunits and ends to the north in a relatively shallow graben between the Cookes Range and the Goodsight Mountains. South of I-10, it includes a deep half graben that is tilted eastward toward the Camel Mountain footwall block near the International Boundary (Mesquite Lake subbasin of Seager, 1995). The 9435-ft Skelly No. 1A, NM "C" oil and gas exploration well in the deepest part of the hanging-wall block encountered 5064 ft of basin fill, with all but the upper 700 ft comprising well-consolidated Middle and Lower Gila/Santa Fe group fanglomerate, sandstone and siltstone. Precambrian basement was encountered at 8794 ft, below a thin, faulted sequence of Lower Paleozonic rocks and a thick section of Eocene and Oligocene volcanic rocks. The upper basin-fill sequence is dominated by fluvial-deltaic deposits of the ancestral Mimbres River (Love and Seager, 1996) that grade into lake and playa deposits near the U.S.-Mexico border (see Stop 2 discussion). Poor ground-water quality and alkaline soil conditions in much of the Florida subbasin area south of I-10 have resulted in limited exploitation of aquifers relative to the Deming subbasin west of the Florida uplift (Hanson et al., 1994; Hawley et al., 2000). **1.0**

23.3 Junction with dirt road at mouth of Victorio Canyon. **Turn left** (north). **0.2**

23.5 Junction with dirt road on left. **Continue on the right fork**. **0.3**

23.8 Junction with dirt road on left. **Continue on the right fork** (mine dump on the left). **0.1**

23.9 Pass through gate. **0.1**

24.0 **Sharp left turn**; Junction with dirt road on right. **Continue left** to the south of the Three Little Hills. **0.4**

24.4 Junction with dirt road on left. **Turn right** (north). **0.2**

24.6 Junction with dirt road on left. **Take right fork**, staying on main dirt road. **1.7**

26.3 Cattle guard. **2.0**

28.3 Road junction, **keep left** (straight). Little Florida Mountains at 2:00. **0.3**

28.6 Road junction, **keep right** (straight). **0.1**

28.7 Cattle guard. **0.1**

28.8 Cattle guard. **0.7**

29.5 Top of ridge; begin descent into arroyo. Cookes Peak at 12:00. **1.0**

30.5 Fork in road; **take right fork**. **0.2**

30.7 Cross cattle guard. Junction with dirt road on right; **continue straight**. **0.3**

31.0 **Sharp right bend** in road at brick ranch house. **1.4**

32.4 Junction with gravel road with NM-198 at stop sign. **Continue straight** onto paved road (NM-198). **0.7**

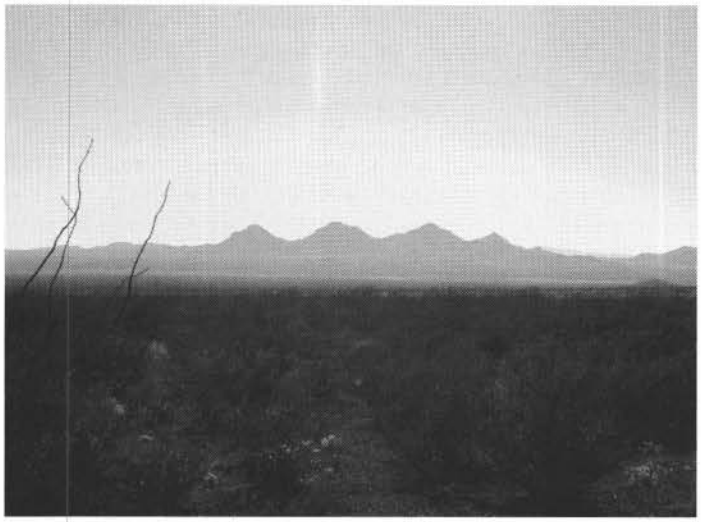

FIGURE 3.13. Tres Hermanas Mountains, looking southwest from the southern Florida Mountains.

33.1 Junction with NM-198 with NM-143. **Turn left** onto NM-143. Red Hill at 10:00; Cookes Peak at 12:00; Rockhound State Park at 3:00; Black Mountain at 11:00. **1.9**

35.0 Junction with NM-143 with NM-141. **Turn left** (west) onto NM-141. **0.3**

35.3 Cross West Florida Mountain fault zone. Continue west across Deming subbasin of the Mimbres basin system. The three-dimensional hydrogeologic framework of this area (to about road log mi 48.5) was originally described by Darton (1916). **4.0**

39.3 O'Kelly Sand and Gravel pits and Desert Valley Sand and Gravel pits to the left. **1.9**

41.2 Junction of NM-141 with NM-11 (Columbus Road) at stop sign. **Turn left** onto NM-11 and continue south (to road log mi. 54.0) on western part of the fluvial-fan complex of the ancestral Mimbres River (Love and Seager, 1996). Tres Hermanas Mountains at 12:00 (Fig. 3.13). **4.0**

THE TRES HERMANAS MINING DISTRICT, LUNA COUNTY, NEW MEXICO

Virginia T. McLemore

New Mexico Bureau of Mines and Mineral Resources, New Mexico Institute of Mining and Technology, 801 Leroy Pl., Socorro, NM 87801; ginger@gis.nmt.edu

The Tres Hermanas district in the Tres Hermanas Mountains near Columbus, in southern Luna County, was discovered in 1881. Total production from skarn and vein deposits in the district is unknown, but is estimated from 1885–1957 as $1,000,000 worth of zinc, lead, silver, gold, and copper, including 1 million lbs Zn, 200,000 lbs Pb, 4000 oz Ag, 7 oz Au, and 550 lbs Cu (McLemore et al., 1996b). The Cincinnati, Hancock, and Mahoney mines were active in 1905 (Lindgren et al., 1910) and the Mahoney mine remained in production until 1920 (Griswold, 1961). In 1906–1907, ore was shipped to the Mississippi Valley area for smelting (Lindgren, 1909). The results of exploratory drilling in the early 1980s are unknown. A hole was drilled in 1997, but no mineralized zones were encountered.

The Tres Hermanas Mountains consist predominantly of a quartz monzonite stock that is surrounded by a thick sequence of predominantly Paleozoic and Cretaceous sedimentary rocks and Tertiary volcanic rocks (Fig. 3.14; Balk, 1962; Griswold, 1961; Leonard, 1982).

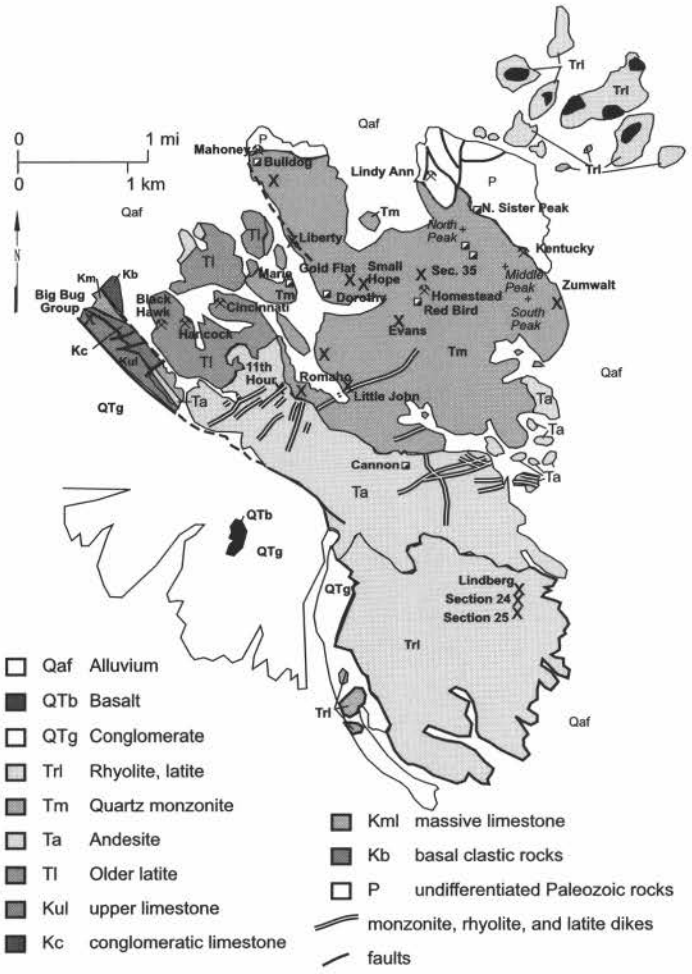

FIGURE 3.14. Simplified geologic map showing major mines in the Tres Hermanas mining district, New Mexico (simplified from Balk, 1962).

The quartz monzonite has been dated as 34.57 ± 0.51 Ma ($^{40}Ar/^{39}Ar$, hornblende, Fig. 3.15). Thrust faults are common; in the West Lime Hills, Permian rocks are thrust over Lower Cretaceous rocks (Drewes, 1991). Much of the Paleozoic limestone near the quartz monzonite stock has been metamorphosed (Homme, 1958; Homme and Rosenzweig, 1970). A chemical variation with time from older metaluminous andesite, dacite, and rhyolite to younger alkaline rhyolite and latite occurs in the calc-alkaline rocks in the Tres Hermanas Mountains (Leonard, 1982). Basaltic dikes locally intruded the quartz monzonite and Permain and Cretaceous rocks.

Two types of deposits, veins and skarns, occur in the Tres Hermanas district. The age of the mineral deposits is Tertiary; they most likely formed after intrusion of the quartz monzonite but prior to intrusion of basaltic dikes (Griswold, 1961; Doraibabu and Proctor, 1973). Geochemical data are consistent with a source of mineralization from the quartz monzonite, although locally the older bedrock may have contributed metals (Doraibabu and Proctor, 1973). Multiple periods of mineralization are likely, as suggested by variation in mineralization style and alteration.

The most productive deposits are the skarn occurrences in the Escabrosa Limestone (Mississippian) and overlying Pennsylvanian sedimentary rocks. Tabular to pod-shaped skarns, commonly silicified, are controlled by fractures and faults, which trend east–west and north–south. Skarns are locally common in limestone xenoliths in the quartz monzonite and in limestone adjacent to the stock. Ore minerals consist predominantly of sphalerite, galena, chalcopyrite, willemite, calamine, smithsonite, and other oxidized lead-zinc minerals in a gangue of calcite, quartz, pyrite, and calc-silicate minerals (Lindgren et

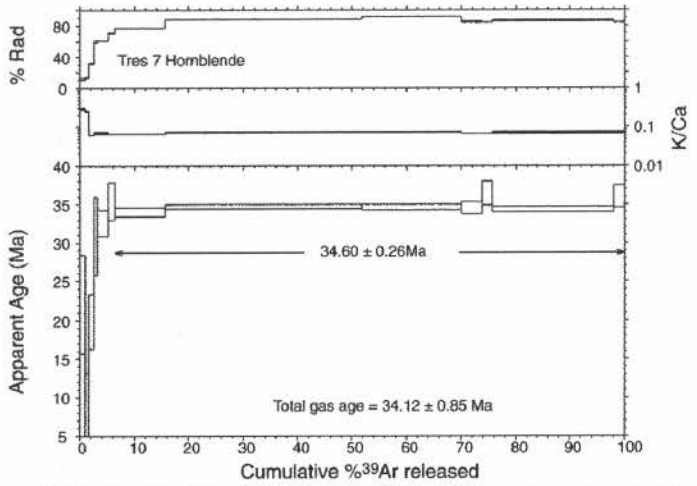

FIGURE 3.15. $^{40}Ar/^{39}Ar$ apparent age spectrum for quartz monzonite from the Tres Hermanas Mountains ($^{40}Ar/^{39}Ar$, hornblende, New Mexico Geochronology Laboratory, New Mexico Institute of Mining and Technology).

al., 1910; Wade, 1913; Homme and Rosenwieg, 1970). Ore at the Mahoney mine averaged 26.7% Pb, 34.5% Zn, and 5.9 oz/short ton Ag. Gold assays range as high as 1500 ppb Au (Griswold et al., 1989). The Mahoney and Lindy Ann mines are the largest producers. Scheelite is reported in a tactite near South Peak (Griswold, 1961).

Fissure veins in quartz monzonite contain galena, willemite, smithsonite, and hydrozincite, and samples assayed 29–37% Zn, 11–40% Pb, and 68.5 ppm Ag (Lindgren, 1909). Veins also occur along faults and fractures in Paleozoic sedimentary clastic rocks, quartz monzonite, and Tertiary volcanic rocks. The most productive veins, such as the Cincinnati, trend east–west; the north-trending veins have been less productive (Doraibabu and Proctor, 1973). The Cincinnati vein strikes N75°E, dips 75–80°S, and is 10,000 ft long. Most veins are less than 4 ft wide. Disseminated pyrite, chalcopyrite, sphalerite, and galena occur sporadically throughout the quartz-monzonite stock, suggesting the potential for a porphyry-copper and/or copper-molybdenum deposit; although the stock is not as extensively altered as typical porphyry-copper deposits. Drilling in the stock has failed to reveal any economic concentrations (Griswold, 1961; NMBMMR file data).

Most of the mines in the Tres Hermanas district are shallow; only a few reach depths of 92–153 m. None of the deposits have been explored at greater depths, especially in the Mahoney and Cincinnati mines (Griswold, 1961). Areas of pyrite disseminations need examination, for example secs. 26, 27, T27S, R9W. Wherever alluvium covers the extensions of these deposits is also favorable, but requires drilling.

Locally, marble occurs adjacent to the quartz monzonite surrounding the Tres Hermanas Mountains (Griswold, 1961; Leornard, 1982). The marble was originally Paleozioc limestone and dolostone and is medium–coarse grained with local, intercalated bands of garnet. The quantity of resources of marble for dimension stone is unknown. Yellow and white travertine (Mexican onyx) occurs in bands as much as 5 ft thick in latite on the southern slopes of the Tres Hermanas Mountains (sec. 24, T28S, R9W) and could be mined for local use. Spurrite, a rare pale-gray–purple mineral valued by collectors and used as an ornamental stone, occurs in a limestone xenolith in quartz monzonite on the east slope of South Sister Peak (Griswold, 1961).

45.2 Junction ahead with NM-332; **continue south** on NM-11. Sunshine School and community center to right. This part of the Deming subbasin is near the center of greatest stress on the shallow basin-fill aquifers due to groundwater mining during the past century. Resultant land subsidence and earth-fissure formation first came to the attention of hydrogeologists in the early 1980s, but the process was probably noted by local residents several decades earlier. Studies of aquifer deformation, land subsidence, and earth-fissure formation due to irrigation-well production in this immediate area have been described by Cantaldo and Mueller (1988) and Haneberg and Friesen (1995). **3.3**

48.5 Road curves to left; junction ahead with NM-517. **Continue southeast** on NM-11. **1.0**

49.5 Gravel pits ahead on left in distributary channel deposits of the ancestral Mimbres fluvial-fan system.

53.1 MP-18. **Be prepared to turn left 0.9 mi ahead. 0.9**

54.0 Junction of NM 11 with CO72 (road sign is on CO72 to the west). **Turn left** (east) onto CO72, through gate and over cattle guard. Route ascends distal piedmont slope of the southwestern Florida Mountains. For approximately the first mile, alluvial-fan deposits of middle–late Quaternary age have a discontinuous veneer of eolian sand and silt. The road passes through the Florida Mountains Wilderness Study Area. **Please drive only on established roads. 1.6**

55.6 Cattle guard. Junction with dirt road on right. **Continue straight** toward the southern end of the Florida Mountains. Within a mile to the east (near power line crossing), the route crosses a break in slope in the gravity gradient away from the Florida uplift (bouguer anomaly map in Seager, 1995). This gravity inflection marks the approximate position of the southwestern range-boundary fault zone according to Seager (1995; his Snake Hills fault zone). A northern branch of this zone appears to merge with the West Florida Mountain fault about 3.1 mi east of road log mi 48.5. **1.7**

57.3 Road junction, **keep left. 0.2**

57.5 **STOP 2.** Magma mixing in the Florida Mountains intrusion. From the parking loop, walk north into the drainage, then west along the drainage and north up into the canyon. The most dramatic magma-mixing sites are farther to the north, but there are excellent examples of mixed magmas exposed in boulders in the drainages.

Magma mixing is an important process in the evolution of igneous rocks. It occurs when magmas of different compositions encounter each other during transport in the crust. Field relationships suggest that it is common to have mafic magmas (now represented by diorite enclaves) penetrate a silicic magma chamber (now represented by the granites of the intrusion), as happened here in the Florida Mountains. The presence of orthoclase and quartz phenocrysts in the granite and lack of phenocrysts in the diorite suggests that the granite was partially molten at the time of mixing, but that the dioritic magma was mostly or completely liquid. Because the crystallization temperature of the mafic magma was higher than that of the granite, the mafic magma froze into "pillows" against the cooler silicic magma. These semi-rigid pillows often broke open and spilled fresh mafic magma into the granite, generating several generations of mixed magmas.

The mafic enclaves previously have been interpreted as hornfels xenoliths from the country rock; however, several lines of evidence suggest that they do indeed represent mixing of mafic and silicic magmas that were produced in the same tectonic event. Chilled pillow margins (Fig. 3.16) and the presence of coarser-grained granite surrounding the pillow (Fig. 3.17) suggest that

FIGURE 3.16. Examples of mixed magmas in rocks near the parking area at Stop 2. Note the crenulate margin between the light and dark magmas near the top of the diagram and the large K-feldspar xenocrysts in the mafic enclave in the center of the diagram. Scale is 2.5 in. long.

the mafic magma quenched against the granite and that the heat released during crystallization caused growth of crystals adjacent to pillow walls. Xenocrysts of orthoclase completely surrounded by diorite match the texture of orthoclase phenocrysts in the granite, and could not exist inside mafic enclaves if the enclaves had been incorporated as solid rocks (Fig. 3.16). The diorite-granite contact in many areas is conspicuously crenulate (Fig. 3.18), a feature frequently observed at liquid-liquid interfaces. In addition, the incompatible trace-element pattern of diorites is similar to those of granites and syenites in significant ways. For instance, both lithologies have nearly the same chondrite-normalized abundances of Ta and La (Fig. 3.11), indicating that neither magma was produced in a continental arc, but rather that they are rift- or plume-related. Furthermore, major element trends of texturally hybrid rocks plot on a linear trend from the most-mafic enclave to the silicic mixing end-member on the fractionation trend of the intrusion (Fig. 3.10).

The parking area for this stop offers a panoramic view of much of the southern Mimbres basin system, which merges southwestward with the Bolson de los Muertos in Chihuahua. The Tres Hermanas Mountains to the south-southwest are erosional remnants of Oligocene quartz-monzonite stocks intruded into Paleozoic and Cretaceous sedimentary rocks (Seager and Clemons, 1988: McLemore, this volume, p. 40). Lower–middle Tertiary volcanic and sedimentary rocks are also a major component of this complex fault-block uplift between the Hermanas subbasin to the west, and the Columbus subbasin to the east.

The narrow gap in the foreground between the Florida uplift and the Greasewood Hills section of the Tres Hermanas Mountains is underlain by no more than 984 ft of Gila Group basin fill which overlies Upper Oligocene–Lower Miocene(?) basaltic andesites (Blandford and Wilson, 1987; Seager, 1995; Hawley et al., 2000). The confluence of the ancestral Mimbres River (Pliocene–early Holocene?) with Seventysix

FIGURE 3.17. Mixed magmas in the southern Florida Mountains.

Draw (Palomas Creek of Darton, 1916, 1917) is located in this gap. The drainage basin of the latter stream system includes the southeastern slopes of the Big Burro uplift and much of the northern slope of the Cedar Mountain Range (see Day 2 Road Log, mileage 113.1–117.4).

Ground water that is not captured by irrigation and urban-industrial uses in the deep Deming subbasin spills through the "Tres Hermanas-Florida" gap into the Columbus subbasin and adjacent parts of the Florida subbasin to the east. It is ultimately discharged as underflow to the Bolson de los Muertos area prior to development of intensive irrigation agriculture in the Columbus and Hermanas areas. Important aquifers near Columbus and Palomas (Chihuahua) include not only fluvial sand and gravel of the Upper Gila Group (Mimbres Formation correlatives), but also Upper Miocene(?) and Pliocene basalts of the Palomas volcanic field, which is located along and south of the International Boundary between the Hermanas and Columbus (Palomas) subbasins.

The upper basin-fill section in the Columbus-southern Florida subbasin area includes thick fine-grained clay deposits (Blandford and Wilson, 1987; Hawley et al., 2000) that document the presence of extensive lakes in the Bolson de los Muertos and Lower Rio Casas Grandes basin in cooler and wetter parts of the

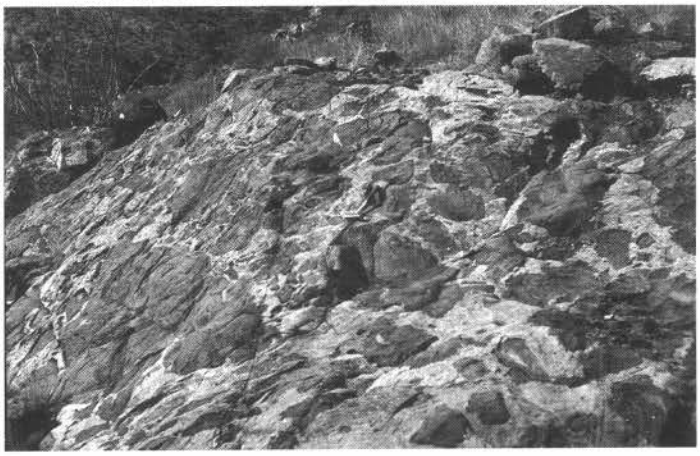

FIGURE 3.18. Mixed magmas in the southern Florida Mountains.

Pleistocene and probably also Pliocene time (Hawley, 1969, 1993; Morrison, 1969; Reeves, 1969). The latest interval of deep-lake formation occurred during the Wisconsin (glacial) Stage. At its highest shoreline level (about 4018 ft), pluvial Lake Palomas of Reeves (1969) had an area of approximately 3000 mi^2 and extended a short distance into New Mexico at the lower end of the ancestral Mimbres fan-delta system (Love and Seager, 1996).

Retrace route back to NM-11. **2.2**

59.7 Cattle guard and junction with dirt road on left. **Continue straight** west towards NM-11. **1.6**

61.3 Junction of CO72 with NM-11. **Turn right** (north) on NM-11 to reach Deming. **Turn left** (south) to reach Columbus.

End of Third-day Road Log.

PANCHO VILLA STATE PARK

Virginia T. McLemore

New Mexico Bureau of Mines and Mineral Resources, New Mexico Institute of Mining and Technology, 801 Leroy Pl., Socorro, NM 87801; ginger@gis.nmt.edu

Pancho Villa State Park in Columbus, New Mexico, was established in 1959 "in interest of preservation of the memory of the unique, historical occasion of the last hostile action by foreign troops within the continental United States" (Kottlowski, 1980). It became the only park in the United States to be named after a foreign invader (Julyan, 1996). The creation of the 60-acre park was a gesture of good will between the United States and Mexico. The town of Columbus has been designated a National Historic Site. Across the street from the park is the privately owned Pancho Villa museum.

Visitors enjoy camping, hiking, picnicking, and wildlife viewing; campsites, restrooms with showers, a dump station, group shelters, and a playground are available. Bird watching is also a favorite pastime. Many of the camp sites offer full hookups that are designed especially to attract winter visitors. Interpretive hiking trails wind through the park, providing visitors a chance to view 30 different species of desert cacti and other flora in the botanical gardens, as well as historical exhibits from Camp Furlong. The park's visitor center was originally the U.S. Customs House and was built in 1901. At the center, visitors can enjoy exhibits describing Pancho Villa's raid and Pershing's Punitive Expedition. A film is shown regularly.

The desert surrounding Columbus was never very attractive to anyone before 1891. Very few people traveled through the area and no one settled here. Water is scarce, summers are hot, and the wind blows constantly. The area is still remote and somewhat desolate.

In 1848, the Mexican War ended with the signing of the Treaty of Guadalupe Hidalgo, and New Mexico became part of the United States of America. The International Border between Mexico and New Mexico was to be settled later by a special commission comprising representatives from both countries. In 1850, President John Taylor appointed John Russell Bartlett as the head commissioner and assigned him to establish and map this southern boundary (Clemons et al., 1980). The original map from the treaty was found to be in error, but the Mexican representative, General Pedro Garcia Conde nevertheless suggested that the flawed map be accepted. Bartlett proposed a compromise that would have established the boundary 40 mi north of Columbus, thereby placing Columbus and Deming in Mexico. Bartlett's compromise was not received well in Washington and he was recalled. Congress wanted this stretch of land, the Mesilla strip, to complete the transcontinental railroad. President Franklin Pierce appointed James Gadsen to correct the compromise and negotiate a settlement. On April 25, 1854, the Gadsen Treaty was signed and the disputed Mesilla strip became part of the Gadsen purchase and ultimately the United States.

Colonel Andrew O. Bailey originally founded Columbus, New Mexico in 1891. Bailey chose the site in hopes of it becoming a point of entry for a planned Northern Mexican and Pacific Railroad that would connect Mexico with the United States. That railroad was never built. However, in 1902 the El Paso and Southwestern Railroad built a railroad connecting El Paso, Texas and Douglas, Arizona, and also built a depot north of the community of Columbus. Soon the town moved to the depot. Luna County was established in 1901 from parts of Grant and Doña Ana Counties with the county seat at Deming, north of Columbus. Camp Furlong was established at Columbus early in 1916 to protect the border region against raids from Mexico as a result of the Mexican Revolution that started in 1910.

On March 9, 1916, Pancho Villa and approximately 500 men raided, burned, and looted the small town of Columbus. By daylight, the end of the raid, ten U.S. civilians and eight soldiers were killed; two civilians and two soldiers were wounded. At least 90 of Villa's men were killed and many more wounded; some accounts claim that more than 200 of his men were killed (McGraw, 1988).

Many reasons have been given for the raid. Villa was involved in the Mexican Revolution and was short on supplies, ammunition, and guns. He felt betrayed by President Woodrow Wilson, who at one point had supported Pancho Villa, but later switched his support to the Mexican government, led by Venustiano Carranza. Wilson allowed approximately 3000 Mexican government soldiers to travel in the United States from Texas to Arizona to surprise and attack Pancho Villa. Finally, Sam Ravel, a merchant in Columbus, refused to acknowledge a credit Villa believed he had with the storeowner. When one of Villa's men approached Ravel for guns and ammunition in exchange of the credit owed to Villa, Ravel threw him out of his store. Pancho Villa then turned his troops toward Columbus. Fortunately for Ravel, he was out of town on March 9, 1916. Some accounts suggest that Pancho Villa may have been a German sympathizer and the German government encouraged the raid (McGraw, 1988).

Word of the raid was telegraphed across the country. The U.S. Army immediately began pouring men and supplies into Deming and then Columbus. Six days later, General John J. (Black Jack) Pershing, supported by a fleet of four-wheel drive Nash and Jeffry automobiles and eight biplanes, led a punitive force of 10,000 men into Mexico after Pancho Villa. Villa's forces were scattered throughout Chihuahua, Mexico; Pershing's men found and killed more of Villa's men and recovered most of the stolen guns and ammunition. Pershing returned to the United States 11 months later when the Mexican government requested that the Americans leave Mexico.

Although Pancho Villa was not caught, the Punitive Expedition into Mexico provided the military with training and experience that later proved invaluable in World War I. This was the last cavalry action and the first use of motor vehicles and airplanes in a military action by the U.S. Army. Sometimes the vehicles had to be dismantled and both they, and much of the fuel, were transported by pack animals and wagons! The first grease rack installed to service U.S. Army vehicles is near the headquarters building at the park (Kottlowski, 1980). The first airbase used for combat was established at Columbus. Photojournalism was used throughout the campaign and was perfected at this time.

After the Punitive Expedition, the soldiers returned home and the town of Columbus soon became nearly deserted. Camp Furlong closed in 1924. In the early 1960s, the railroad near Columbus was abandoned. Today, Columbus is a small, quiet community dependent on ranching, farming, retirees, and travelers. The international border crossing between Columbus and Palomas, Mexico is open 24 hours a day.

The most prominent topographic feature within the park is Villa Hill (also known as Cootes Hill), in the northwest corner. This hill rises approximately 25 ft above the flat, featureless desert floor and is composed of reddish-brown–black, vesicular basalt. Small xenoliths or fragments of limestone and other country rock are found within the basalt. A sample of the basalt was dated by $^{40}Ar/^{39}Ar$ at 3.8 ± 0.6 Ma (groundmass, W. McIntosh, personal commun., 1999; Fig. 3.19). A sample of a similar lava flow southwest of Columbus has been dated at 3 Ma (Seager et al., 1984). Geochemically, the Pancho Villa basalt is alkaline and similar in chemical composition to the basalt found in the Potrillo

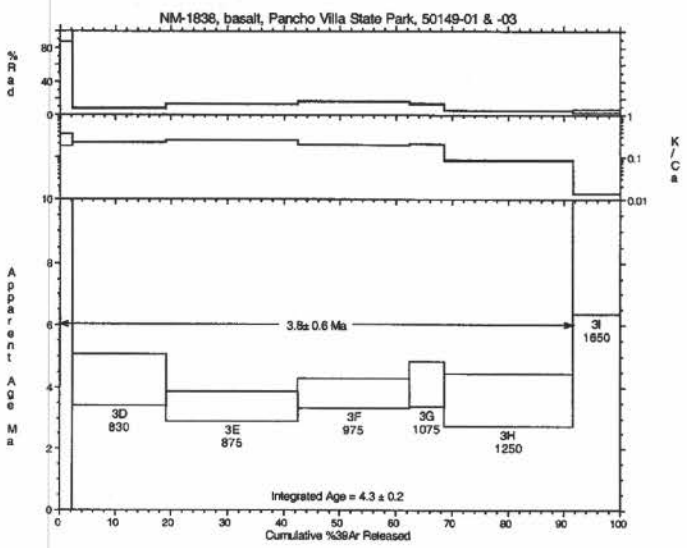

FIGURE 3.19. $^{40}Ar/^{39}Ar$ apparent age spectrum for basalt from Pancho Villa State Park.

volcanic field south of Las Cruces and east of Columbus. The basalt was formed by partial melting of material derived from the upper mantle (Anthony et al., 1992) and was extruded during the latest stages of the formation of the Rio Grande rift (Seager et al., 1984; McLemore, 2000).